T.R.
BOLU ABANT İZZET BAYSAL ÜNİVERSİTESİ
INSTITUTE OF GRADUATE STUDIES
DEPARTMENT OF CHEMISTRY

INVESTIGATION OF THE IMPACT OF COBALT ION DOPING ON THE SYNTHESIS AND STRUCTURE OF MAGNESIUM ORTHOBORATE CERAMIC POWDERS

MASTER OF SCIENCE, CHEMISTRY

BETÜL YILDIRIM

ACADEMIC SUPERVISOR
Prof. Dr. Ayşe MORKAN
. CO-SUPERVISOR: DR. ESRA GÖĞCEGÖZ

BOLU, 4/9/2025

ACCEPTANCE AND APPROVAL PAGE

The thesis entitled **INVESTIGATION OF THE IMPACT OF COBALT ION DOPING ON THE SYNTHESIS AND STRUCTURE OF MAGNESIUM ORTHOBORATE CERAMIC POWDERS** was presented and submitted by **Betül YILDIRIM** in partial fulfillment of the requirements for the degree of **Master of Science** in Department of **CHEMISTRY** with majority vote is hereby approved. 4/9/2025

Jury Members	**Signature**
Supervisor Prof. Dr. Ayşe MORKAN Bolu Abant Izzet Baysal University	.....
Member Prof. Dr. Fazilet Devrim ÖZDEMİRHAN Bolu Abant Izzet Baysal University	.....
Member Prof. Dr. Mecit AKSU Düzce University	.....

Institute of Graduate Studies Approval

Prof. Dr. İbrahim KÜRTÜL

Director of Institute of Graduate Studies

ETHICAL DECLARATION

In this thesis study, which I have prepared in accordance with the Bolu Abant İzzet Baysal University, Institute of Graduate Studies' Thesis Writing Guide and Template:

- I have obtained the data, information, and documents presented in the thesis within the framework of academic and ethical rules.
- I have presented all information, documents, evaluations, and results in accordance with the rules of scientific ethics and morality.
- I have cited and referenced all the works I have benefited from in the thesis study.
- I have not made any changes to the data used.
- I declare that the work I have presented in this thesis is original, and in any other case, acknowledge and accept any potential loss of rights that may arise against me.

According to the similarity report obtained by applying the filters determined by the directorate of the institute in the Turnitin program related to the thesis, the similarity index of the thesis does not exceed 30%.

.....

BETÜL YILDIRIM

PREFACE

This thesis represents the culmination of my extensive research and academic endeavors over the past years. It centers on the Investigation of the Impact of Cobalt Ion Doping on the Synthesis and Structure of Magnesium Orthoborate Ceramic Powders—a subject of both personal relevance and scientific significance. The insights and findings presented herein are the result of countless hours of rigorous experimentation, meticulous analysis, and critical reflection.

ABSTRACT

INVESTIGATION OF THE IMPACT OF COBALT ION DOPING ON THE SYNTHESIS AND STRUCTURE OF MAGNESIUM ORTHOBORATE CERAMIC POWDERS
MSC THESIS
BETÜL YILDIRIM
BOLU ABANT IZZET BAYSAL UNIVERSITY
INSTITUTE OF GRADUATE STUDIES
DEPARTMENT OF CHEMISTRY
(SUPERVISOR: PROF. DR. AYŞE MORKAN)
(CO-SUPERVISOR: DR. ESRA GÖĞCEGÖZ)
BOLU, 9 APRIL 2025
x+ 28 pages

In this thesis, the synthesis of undoped and cobalt ion doped nanosized magnesium orthoborate ceramic powders was carried out via conventional solid state synthesis technique. Cobalt-containing magnesium orthoborates were prepared using $Mg(NO_3)_2.6H_2O$, 5% excess H_3BO_3 and cobalt nitrate $Co(NO_3)_2.6H_2O$ as starting materials. Different concentrations of cobalt metal ion were used to obtain the kotoite type of magnesium orthoborate given within the formula $Mg_{3-x}Co_x(BO_3)_2$ (x: 0.005, 0.01, 0.025, 0.05, 0.075, 0.500, 1.000, 1.500, 2.000, 2.500). The impact of different concentrations of cobalt metal on the structural features of the synthesized products was examined by the XRD technique. When the XRD data were examined, it was observed that in the kotoite structured borate materials obtained in the orthorhombic crystal system at 900ºC, the low amount of Co(II) ion added did not cause any change in the crystal structure of the kotoite. However as the cobalt ion content increased, the formation of cobalt orthoborate ($Co_3(BO_3)_2$) has became evident. Additionally, FTIR analysis revealed that all the characteristic bands of orthoborates were observed between 2000–500 cm^{-1}. According to the DRS studies, the absorbance spectra of all compounds showed two bands at 250 and 335 nm. It has been observed that the UV band positions for cobalt containing magnesium orthoborate samples slightly shift to the different wavelengths in comparison with the pure $Mg_3(BO_3)_2$. In addition, the thermal properties of cobalt-containing kotoite-type magnesium orthoborate ceramic powders were examined using TG/DTA techniques, and the presence of an endothermic peak around 1390°C was detected for all orthoborate products prepared in this study.

KEYWORDS: Kotoite, magnesium orthoborate, cobalt ion doping, XRD, FTIR

ÖZET

KOBALT İYONU KATKILAMASININ MAGNEZYUM ORTOBORAT SERAMİK TOZLARININ SENTEZİ VE YAPISI ÜZERİNDEKİ ETKİSİNİN ARAŞTIRILMASI
YÜKSEK LISANS TEZI
BETÜL YILDIRIM
BOLU ABANT İZZET BAYSAL ÜNİVERSİTESİ
LİSANSÜSTÜ EĞİTİM ENSTİTÜSÜ
KİMYA ANA BİLİM DALI
(TEZ DANIŞMANI: PROF. DR. AYŞE MORKAN)
(İKİNCİ DANIŞMAN: DR. ESRA GÖĞCEGÖZ)
BOLU, 9 NISAN 2025
x + 28 pages

Bu tezde, katkısız ve kobalt iyonu katkılı nano boyutlu magnezyum ortoborat seramik tozlarının üretimi, geleneksel katı hal sentez tekniği kullanılarak gerçekleştirildi. Kobalt içeren magnezyum ortoboratlar, başlangıç malzemesi olarak $Mg(NO_3)_2.6H_2O$, 5% fazla H_3BO_3 ve kobalt nitrat $Co(NO_3)_2.6H_2O$ kullanılarak hazırlandı. $Mg_{3-x}Co_x(BO_3)_2$ (x: 0.005, 0.01, 0.025, 0.05, 0.075, 0.500, 1.000, 1.500, 2.000, 2.500) formülü ile verilen kotoit tipi magnezyum boratların elde edilmesinde kobalt metal iyonunun farklı konsantrasyonları kullanılmıştır. Sentezlenen ürünlerin yapısal özelliklerine farklı konsantrasyonlarda kobalt metalinin etkisi, XRD tekniği ile incelenmiştir. XRD verileri incelendiğinde, 900ºC de ortorombik kristal sisteminde elde edilen kotoit yapılı boratlı malzemelerde, düşük miktarda katkılanan Co(II) iyonunun, kotoidin kristal yapısında herhangi bir değişiklik yapmadığı gözlenmiştir. Ancak kobalt iyonu içeriği arttıkça kobalt ortoboratın ($Co_3(BO_3)_2$) oluşumu belirgin hale gelmiştir. Ayrıca FTIR tekniği ortoboratların tüm karakteristik bantlarının 2000–500 cm^{-1} arasında gözlendiğini ortaya çıkarmıştır. DRS çalışmalarına göre tüm bileşiklerin absorbans spektrumları 250 ve 335 nm'de iki bant göstermiştir. Kobalt içeren magnezyum ortoborat örneklerinin UV bant pozisyonlarının saf $Mg_3(BO_3)_2$) ile karşılaştırıldığında farklı dalga boylarına kaydığı gözlemlenmiştir. Ayrıca, kobalt içeren kotoit tipi magnezyum ortoborat seramik tozlarının termal özellikleri de, TG/DTA teknikleri kullanılarak incelenmiş ve bu çalışmada hazırlanan tüm ortoborat ürünleri için 1390°C civarında endotermik bir pikin varlığı saptanmıştır.

ANAHTAR KELİMELER: Kotoit, magnezyum ortoborat, kobalt iyonu katkılama, XRD, FTIR

TABLE OF CONTENTS

Page

LIST OF FIGURES

Page

LIST OF ABBREVIATIONS AND SYMBOLS

XRD: X-ray diffraction

FT-IR: Fourier Transform Infrared Spectroscopy

TG: Thermogravimetry

DTA: Differential Thermal Analysis

UV-Vis: Ultra violet-Visible

DRS: Diffuse Reflectance Spectroscopy

ACKNOWLEDGEMENT

I extend my deepest gratitude to my supervisor, Prof. Dr. Ayşe Morkan, for her outstanding guidance, constructive feedback, invaluable suggestions, and continuous support throughout my master's studies. Working under her supervision has been a privilege, and I greatly value her significant contributions to both my academic and professional growth.

I sincerely thank my co-supervisor Dr. Esra Göğcegöz and Dr. Liska Fadliyani, for their unwavering support. Their expertise have enlightened my research journey and vastly enriched the quality of the work.

At last, I wish to express my heartfelt appreciation to my family and friends for their love, and encouragement, which gave me the strength and motivation to bring this thesis to completion.

.

1. INTRODUCTION

Boron stands out as an extraordinary and intriguing element. Throughout history, it has posed enduring challenges and offered inspiration to both chemists and engineers. Naturally occurring boron has two stable isotopes: B-10, representing 19.78% of its composition, and B-11, making up the remaining 80.22% [1-5]

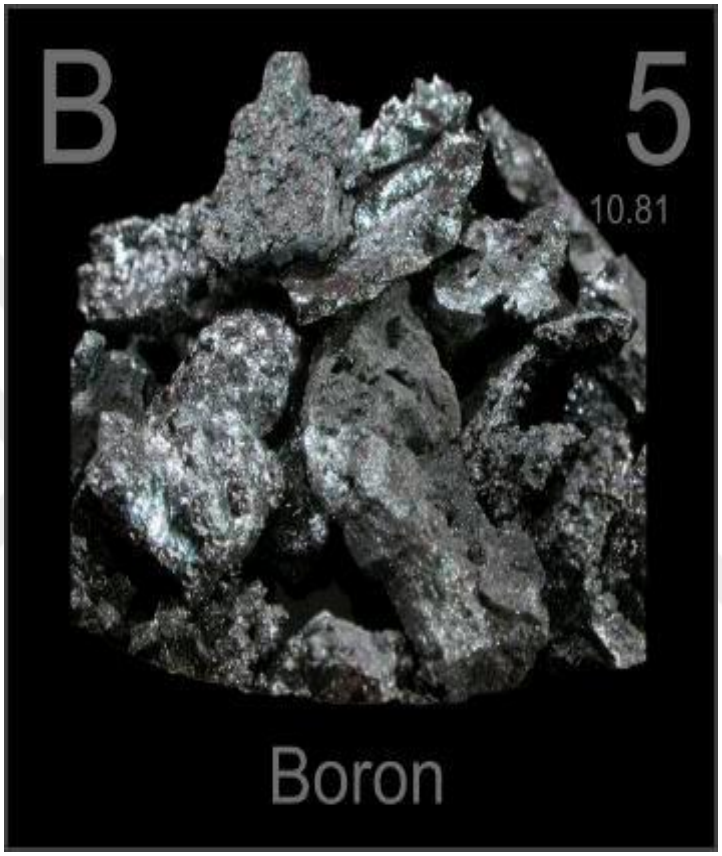

Figure 1.1. Boron

Magnesium Borates	HYDROBORACITE	$CaMgB_6O_{11}.6H_2O$	50,5	Hydroboracite formation is found in Argentina together with Colemanite and it is mainly used in ceramic industry. In addition, it is found in Kazakhstan and Turkey.
	INDERBORIT	$CaMgB_6O_{11}.11H_2O$	41,5	Inder Lake,Kazakhstan
	ASCHARITE (SZAIBÉLYITE)	$MgBO_2OH$	41,4	This mineral formation is mainly used in Kazakhstan and China.
	BORACITE	$Mg_3B_7O_{13}Cl$	62,2	It is frequently found in Emet, Kırka, Bigadiç borate mines. It is seen with colemanite, ulexite and sometimes Tunelite and Vescite-A.
	KURNAKOVITE	$Mg_2B_6O_{11}.15H_2O$	37,3	Inder Lake, Kazakhstan
	INDERITE	$MgB_3O_3(OH)_5•5(H_2O)$	37,3	Inder Lake, Kazakhstan
	SUANITE	$Mg_2B_2O_5$	46,3	Suan, North Korea
	KOTOITE	$Mg_3B_2O_6$	36,5	Bundjiro Koto (1856-1935)
	PINNOITE	$MgB_2O_4.3H_2O$	42,5	Germany and Death Valley, California

Figure 1.2. Boron minerals

Most of the Earth's boron reserves are harbored in Russia, The United States, and Turkey [6].

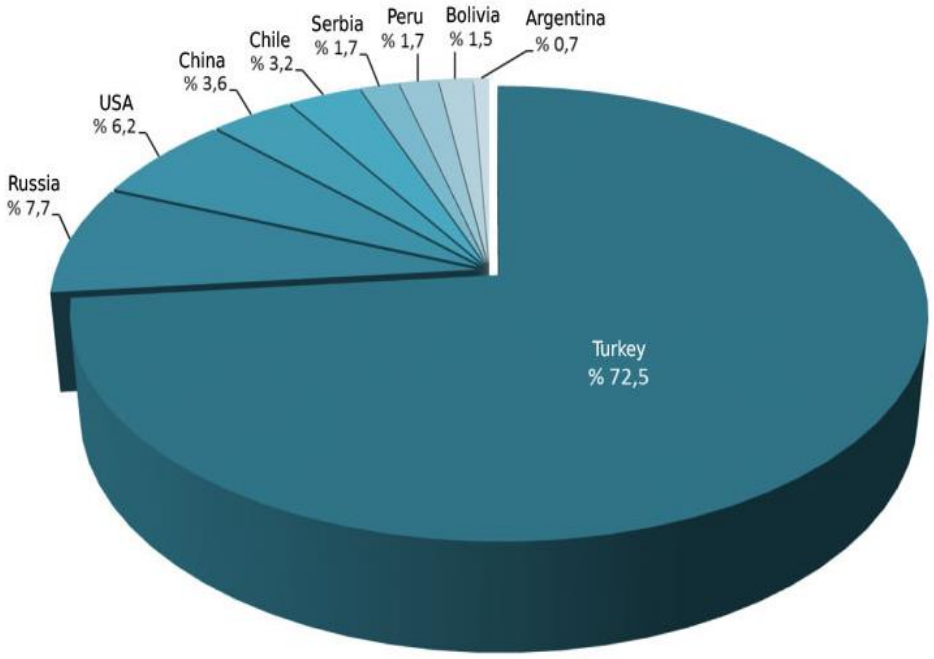

Figure 1.3. Boron Reserves

1.1 Borates

Borates are minerals that contain boric oxide or boron-oxygen molecules. They are the salts of boron's oxyacids, including boric acid (H_3BO_3), metaboric acid (HBO_2), and tetraboric acid ($H_2B_4O_7$). Borates are produced through a boron oxyacid with a base reaction or the interaction of boric acid or boron oxide with a molten metal oxide. The structures of borate anions vary, ranging from the simple trigonal planar BO_3^{3-} ion to more intricate configurations that include chains and rings composed of three- and four-coordinated boron atoms. According to Carpeni, borates are categorized into three groups: (a) ortho- or metaborates, (b) tetraborates, and (c) pentaborates [7].

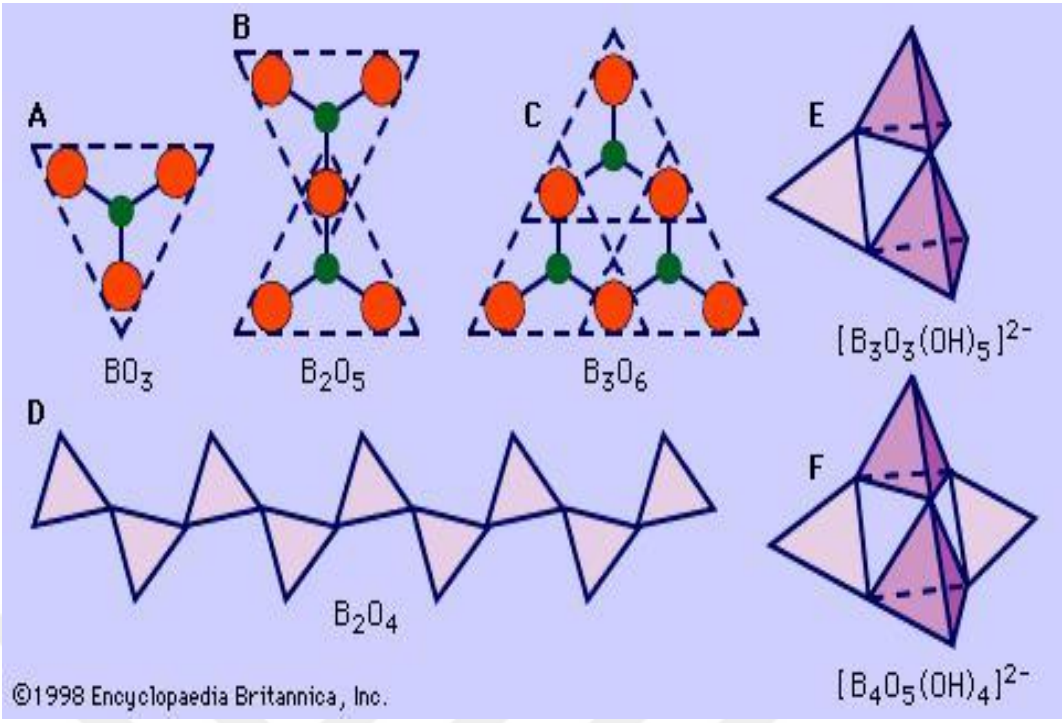

Figure 1.4. Types of borates

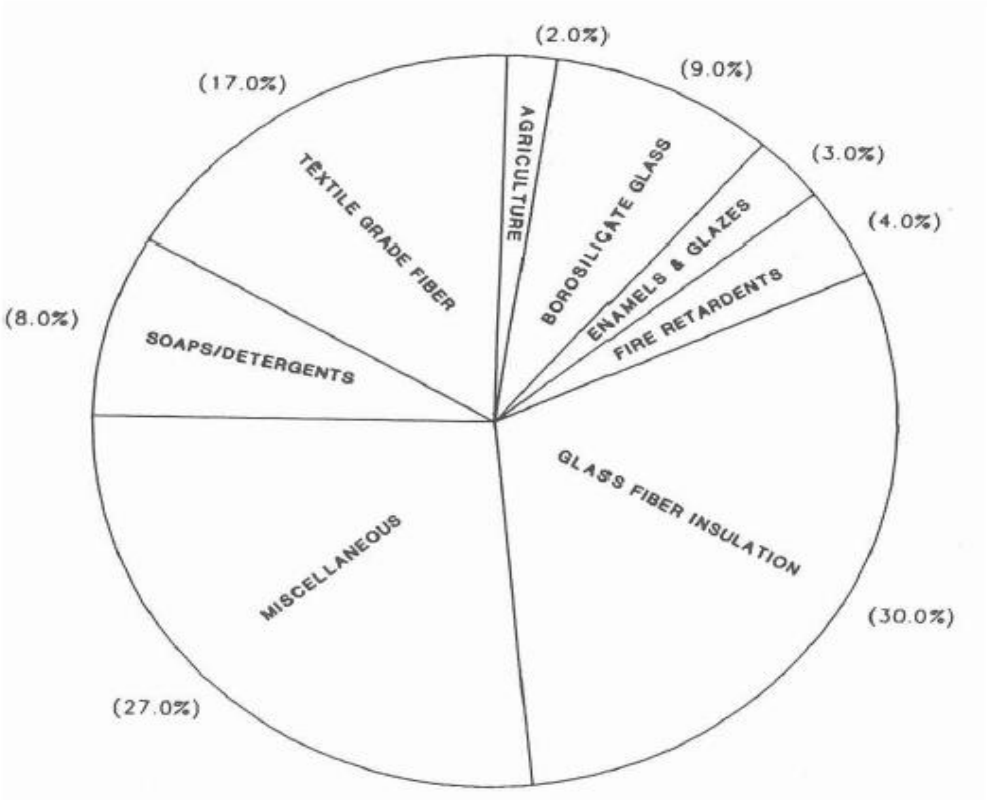

Figure 1.5. The uses of borates

1.1.1 Orthoborates

Orthoborates are salts that contain the ions BO_3^{3-} or BO_4^{5-}. Their structural arrangement is similar to that of nitrates and carbonates. Metal orthoborates generally follow the chemical formula $M_3B_2O_6$ or $M_3(BO_3)_2$, where M can represent elements such as Mg, Ba, Ca, Sr, Ni, Cd, Mn, or Co. In recent years, metal orthoborates have drawn significant attention because of their diverse applications in areas namely electronic ceramics, wide bandgap semiconductors, anti-wear additives, plastics, nonlinear optical devices, magnesium and aluminum matrix alloys, luminescent materials, and laser technologies. Notably, among the numerous orthoborates, only $Mg_3B_2O_6$ (known as kotoite) and $Mn_3B_2O_6$ (referred to as jimboite) have been naturally identified to date [8, 9].

(a)

(b)

Figure 1.6. The minerals of (a) $Mg_3B_2O_6$ (kotoite) and (b) $Mn_3B_2O_6$ (jimboite)

Kotoite, with the chemical formula $Mg_3(BO_3)_2$, features a crystal structure in which each magnesium atom is coordinated by oxygen atoms in an octahedron arrangement. In this arrangement, the oxygen atoms form the vertices of the octahedra, while the magnesium atoms are positioned at their centers. Boron atoms, on the other hand, are located at the center of triangular arrangements formed by oxygen atoms. This structural configuration is depicted in Figure 1.7, where oxygen atoms are represented as small spheres, magnesium atoms occupy the octahedra's center, and boron atoms are located at the centers of the triangular planes [10].

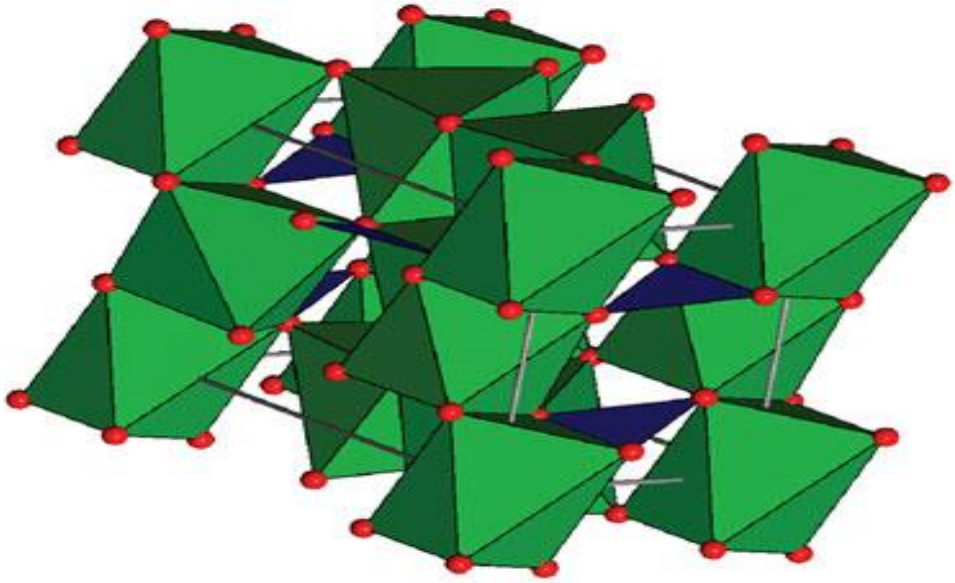

Figure 1.7. The crystal structure of magnesium orthoborates

1.2 Synthesis Methods of Borates

Several methods have been devised to produce high-quality borate compounds. These include approaches like precipitation, hydrothermal techniques, combustion-based synthesis, microwave-assisted methods, conventional solid-state reactions, co-precipitation techniques, spray drying, flux methods, sol-gel processes, mechanochemical strategies solid-state combustion, and solution combustion synthesis. Such techniques, widely utilized for producing powdered ceramics, can generally be grouped into three primary categories: solid-state methods, solution-based approaches, and vapor-phase synthesis [11].

1.2.1 Solid State Reaction Method

Solid-state reactions involve the process of combining powdered solid reactants and applying heat to produce a new solid compound. Common reactants in such processes include metal salts like nitrates, carbonates, sulfates, hydroxides, acetates, alkoxide, and oxalates [12].

The success and efficiency of these reactions are influenced by several factors, such as the chemical properties of the reactants, characteristics of the resulting product, particle size and its distribution, particle shape, uniformity of the

mixture, and external conditions like reaction atmosphere, temperature, and duration of heating.

These reactions offer several advantages, including the use of readily available oxide precursors and cost-effective scalability for industrial powder production. Additionally, they are highly suitable for laboratory-scale synthesis [11-16].

1.3 Purpose of the work

The importance and the aim of this thesis is the preparation and characterization of undoped and cobalt ion doped nanosized magnesium orthoborate ceramic powders as $Mg_{3-x}CoBO_3)_2$ (x: 0.005, 0.01, 0.025, 0.05, 0.075, 0.500, 1.000, 1.500, 2.000, 2.500) by high temperature solid state synthesis method. In the first part of this work, aim is to characterise their crystal structures of Kotoite type of $Mg_{3-x}CoBO_3)_2$ prepared by different concentrations of cobalt metal ion by X-ray diffaraction (XRD) and to investigate the vibrational motions of B-O bonds in triangular BO_3 units by Infrared spectroscopy (FT-IR) technique. In the second part of this study, the other aim is the observation the UV band positions for different concentration cobalt containing magnesium borate compounds and to study their thermal behaviors using TG/DTA. The proposed reactions are given follows;

$(3-x)Mg(NO_3)_2.6H_2O$ (s) + $(x)Co(NO_3)_2.6H_2O$(s) + $2H_3BO_3$(s) → $Mg(3-x)\ Co(x)\ (BO_3)_2$(s) + $6NO_2$(g) + $21H_2O$(g) + $1.5O_2$(g)

(x: 0.005, 0.01, 0.025, 0.05, 0.075, 0.500, 1.000, 1.500, 2.000, 2.500)

2. MATERIALS and METHOD

2.1 Materials

During the preparation process, the chemicals that were used are provided below :

- $Mg(NO_3)_2.6H_2O$, Magnesium nitrate hexahydrate (Merck, 99.50%)
- $Co(NO_3)_2.6H_2O$, Cobalt nitrate hexahydrate (Merck, 99.90%)
- H_3BO_3, Boric Acid (Merck, 99.90%)
- KBr, potassium Bromide for the IR pellets preparation (Merck, 99.90%)

2.2 Solid State Reactions of (3-x) $Mg(NO_3)_2.6H_2O(s)$ + (x)$Co(NO_3)_2.6H_2O(s)$ +2$H_3BO_3(s)$

For each value of x (0.005, 0.010, 0.025, 0.050, 0.100, 0.5, 1.0, 1.5, 2.0, 2.5), stoichiometric quantities of $Mg(NO_3)_2.6H_2O$, $Co(NO_3)_2.6H_2O$ and H_3BO_3 were precisely measured. The materials were finely ground together in an agate mortar to achieve a homogeneous mixture. Each mixture was directly placed into porcelain crucibles, which were then introduced to the furnace for further heating processing [17-21].

- **Heating Process:**

  - The temperature of the furnace was firstly adjusted to 450˚C with a heating rate of 15˚C per minute. The mixture of starting reactants was maintained for 4 hours at this temperature, after which it was removed from the furnace, allowed to cool, and then thoroughly crushed and blended before being returned to the furnace.
  - Then, the temperature was gradually increased to 600˚C with a heating rate of 1˚C per minute and kept at this temperature for 3 hours.
  - Following this heating, the sample underwent four separate heating cycles to 900˚C, with the temperature of the furnace rising at a rate of 1˚C per minute. Each cycle included keeping the sample at 900˚C for 12 hours.

- Finally, the product was allowed to cool down to room temperature at a controlled rate of 1˚C per minute.

2.2.1 The solid state chemical reactions expected for different dopant concentrations for the general reaction;

$(3-x)\ Mg(NO_3)_2.6H_2O\ (s) + (x)Co(NO_3)_2.6H_2O(s) + 2H_3BO_3(s) \rightarrow Mg_{(3-x)}\ Co_{(x)}\ (BO_3)_2(s) + 6NO_{2(g)} + 21H_2O_{(g)} + 1.5O_{2(g)}$

- **The expected reaction when x = 0.005**

$2.995Mg(NO_3)_2{\cdot}6H_2O\ (s) + 0.005Co(NO_3)_2{\cdot}6H_2O\ (s) + 2H_3BO_3(s) \rightarrow$

$Mg_{2.995}Co_{0.005(}BO_3)_2(s) + 6NO_2(g) + 21H_2O(g) + 1.5O_2(g)$

- **The expected reaction when x = 0.010**

$2.990Mg(NO_3)_2.6H_2O(s) + 0.010Co(NO_3)_2.6H_2O(s) + 2H_3BO_3\ (s) \rightarrow$

$Mg_{2.990}\ Co_{\ 0.010}(BO_3)_2(s) + 6NO_2(g) + 21H_2O(g) + 1.5O_2(g)$

- **The expected reaction when x = 0.025**

$2.975Mg(NO_3)_2{\cdot}6H_2O\ (s) + \ 0.025Co(NO_3)_2{\cdot}6H_2O\ (s) + 2H_3BO_3(s) \rightarrow$

$Mg_{2.975}Co_{0.025}(BO_3)_2(s) + 6NO_2(g) + 21H_2O(g) + 1.5O_2(g)$

- **The expected reaction when x = 0.050**

$2.95Mg(NO_3)_2.6H_2O(s) + 0.05Co(NO_3)_2.6H_2O(s) + 2H_3BO_3(s) \rightarrow$

$Mg_{2.950}\ Co_{0.050}(BO_3)_2\ (s) + 6NO_2(g) + 21H_2O(g) + 1.5O_2(g)$

- **The expected reaction when x = 0.100**

$2.900Mg(NO_3)_2.6H_2O(s) + 0.100Co(NO_3)_3.6H_2O(s) + 2H_3BO_3(s) \rightarrow$

$Mg_{2.900}\ Co_{0.100}(BO_3)_2(s) + 6NO_2(g) + 21H_2O(g) + 1.5O_2(g)$

- **The expected reaction when x = 0.5**

$2.5Mg(NO_3)_2.6H_2O(s) + 0.5Co(NO_3)_3.6H_2O(s) + 2H_3BO_3(s) \rightarrow$

$Mg_{2.5}C_{0.5}(BO_3)_2(s) + 6NO_2(g) + 21H_2O(g) + 1.5O_2(g)$

- **The expected reaction when x = 1.0**

$2.0Mg(NO_3)_2.6H_2O(s) + 1.0Co(NO_3)_3.6H_2O(s) + 2H_3BO_3(s) \rightarrow$

$Mg_{2.0}Co_{1.0}(BO_3)_2(s) + 6NO_2(g) + 21H_2O(g) + 1.5O_2(g)$

- **The expected reaction when x = 1.5**

$1.5Mg(NO_3)_2.6H_2O(s) + 1.5Co(NO_3)_3.6H_2O(s) + 2H_3BO_3(s) \rightarrow$

$Mg_{1.5}Co_{1.5}(BO_3)_2(s) + 6NO_2(g) + 21H_2O(g) + 1.5O_2(g)$

- **The expected reaction when x = 2.0**

$1.0Mg(NO_3)_2.6H_2O(s) + 2.0Co(NO_3)_3.6H_2O(s) + 2H_3BO_3(s) \rightarrow$

$Mg_{1.0}Co_{2.0}(BO_3)_2(s) + 6NO_2(g) + 21H_2O(g) + 1.5O_2(g)$

- **The expected reaction when x = 2.5**

$0.5Mg(NO_3)_2.6H_2O(s) + 2.5Co(NO_3)_3.6H_2O(s) + 2H_3BO_3(s) \rightarrow$

$Mg_{0.5}Co_{2.5}(BO_3)_2(s) + 6NO_2(g) + 21H_2O(g) + 1.5O_2(g)$

3. RESULTS

3.1 X-Ray Powder Diffraction (XRD) Studies

In the first part of this work, magnesium orthoborate, $Mg_3(BO_3)_2$ as the products were synthesized using $Mg(NO_3)_2 \cdot 6H_2O$ and 5% excess H_3BO_3 as starting materials. Nitrogen-based borate chemicals commonly used in the chemical industry were fabricated through a convential high-temperature solid-state reaction method in a furnace set at 900°C [21, 23-25]. Hence the synthesis for ortoborates considered throughout in this thesis was carried out through the following reaction, with the materials being subjected to a temperature of 900°C for 48 hours. The XRD pattern of the resulting magnesium orthoborate is depicted in Figure 1.1.

$$3Mg(NO_3)_2.6H_2O_{(s)} + 2H_3BO_{3(s)} \rightarrow Mg_3(BO_3)_{2(s)} + 6NO_{2(g)} + 21H_2O_{(g)} + 1.5O_{2(g)}$$

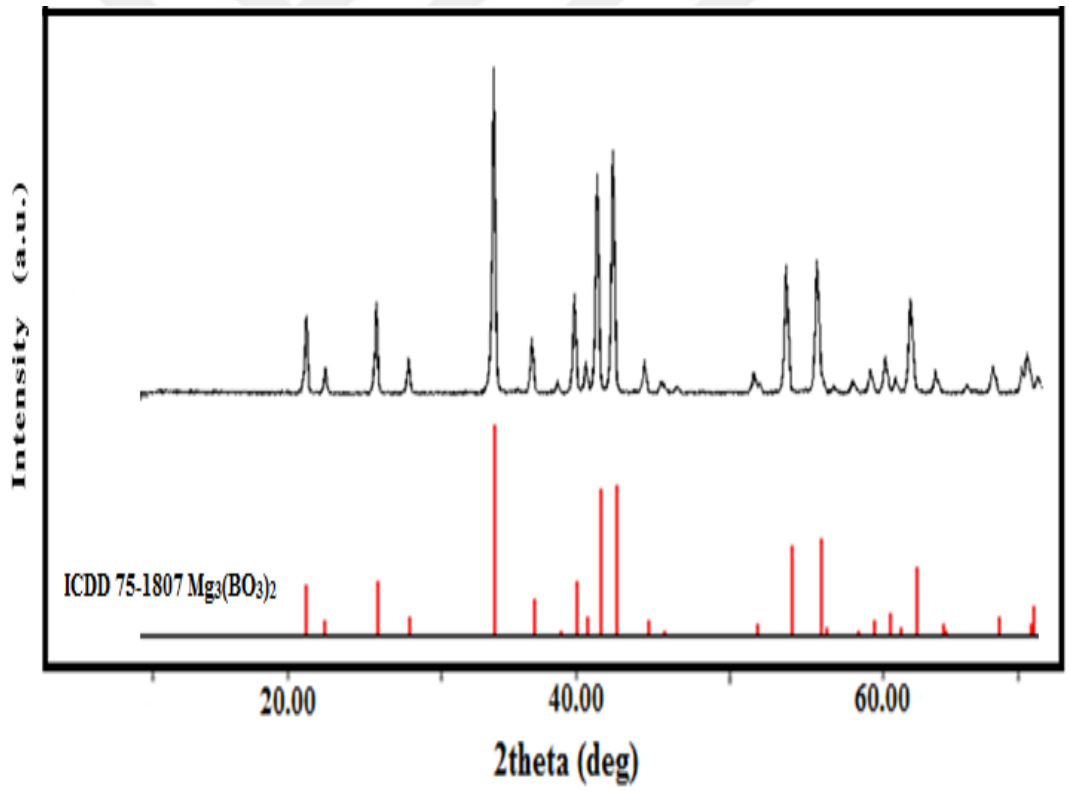

Figure 3.1: XRD patern of $Mg_3(BO_3)_2$

In the continuation of the thesis, cobalt-containing magnesium orthoborates were prepared using $Mg(NO_3)_2.6H_2O$, and 5% excess H_3BO_3 and cobalt nitrate ($Co(NO_3)_2.6H_2O$) as starting materials used in different treatments.

To synthesize Co(II) ion-doped magnesium orthoborate nutrients at the concentrations given in Table 1, the starting materials were individually weighed, crushed, and mixed homogeneously in an agate pestle and mortar. These resulting mixtures were subjected to heat treatment in high temperature furnaces at 900^{o}C for 24 hours and cobalt-containing magnesium orthoborates were synthesized at different concentrations of Co and Mg ions given in Table 1.

Table 1.1 Cobalt concentrations in cobalt-containing magnesium orthoborates

Code	PRODUCTS	Co(II) (%wt.)
F3-4-1	$Mg_{2.995}Co_{0.005}(BO_3)_2$	0.005
F3-4-2	$Mg_{2.990}Co_{0.010}(BO_3)_2$	0.010
F3-4-3	$Mg_{2.975}Co_{0.025}(BO_3)_2$	0.025
F3-4-4	$Mg_{2.950}Co_{0.050}(BO_3)_2$	0.050
F3-4-5	$Mg_{2.925}Co_{0.075}(BO_3)_2$	0.075
C3-4-1c	$Mg_{2.500}Co_{0.500}(BO_3)_2$	0.500
C3-4-2c	$Mg_{2.000}Co_{1.000}(BO_3)_2$	1.000
C3-4-3c	$Mg_{1.500}Co_{1.500}(BO_3)_2$	1.500
C3-4-4	$Mg_{1.000}Co_{2.000}(BO_3)_2$	2.000
C3-4-5	$Mg_{0.500}Co_{2.500}(BO_3)_2$	2.500

The fabricated products were analyzed by XRD and FT-IR techniques. Figure 3.1 illustrates the XRD patterns of the samples prepared with the addition of cobalt ion. Analysis of these patterns revealed that at lower concentrations of cobalt ions, magnesium orthoborate ($Mg_3(BO_3)_2$, ICDD No: 75-1807) was the predominant phase. As the cobalt content increased, the formation of cobalt orthoborate ($Co_3(BO_3)_2$) became evident. Additionally, the intensity of peaks associated with ICDD No: 25-0102 was observed to increase progressively with higher cobalt concentrations.

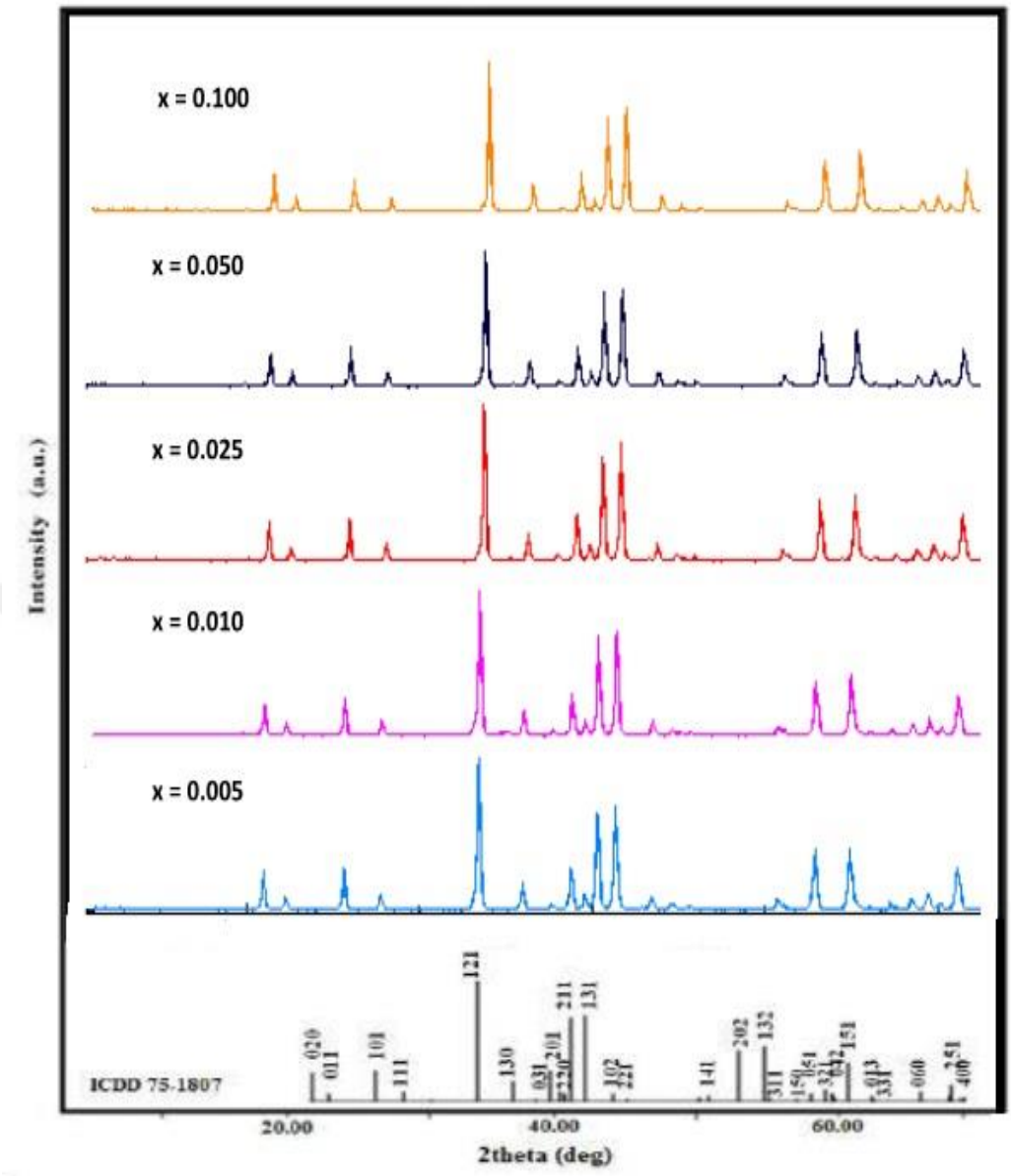

Figure 3.1. XRD Patterns of $Mg_{(3-x)}Co_{(x)}(BO_3)_2$ (x = 0.005 , 0.01 , 0.025 , 0.05 , 0.10) and ICDD 75-1807

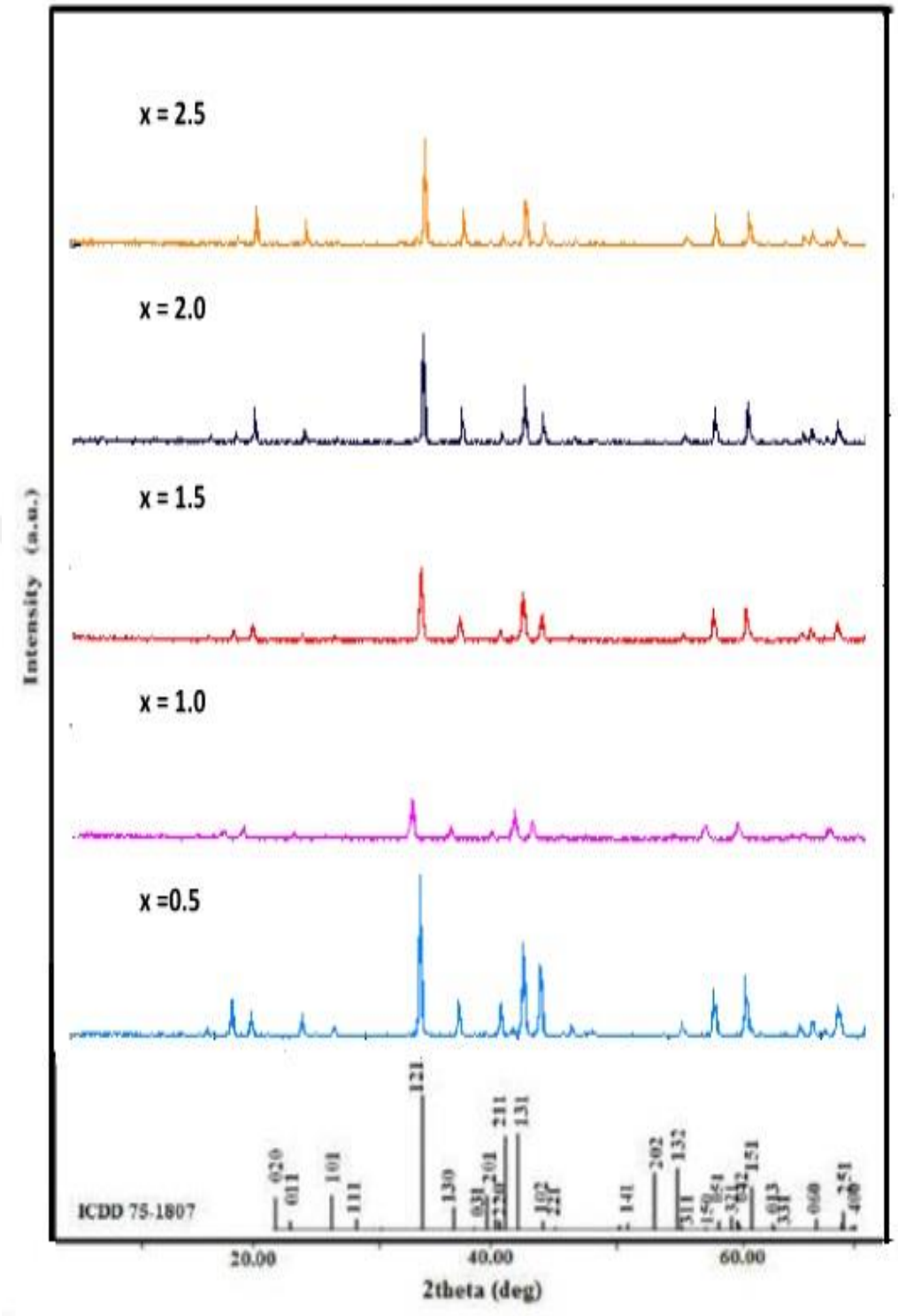

Figure 3.2. XRD Patterns of $Mg_{(3-x)}Co_{(x)}(BO_3)_2$ (x = 0.5, 1.0, 1.5, 2.0, 2.5) and ICDD 75-1807

3.2 Infrared Spectroscopy Studies

The vibrational bands of borates in the FTIR spectra typically appear in the range of 2000–500 cm^{-1}. These bands represent the characteristic bands of the borate network, which can be divided into three distinct regions.

The first region corresponds to the asymmetric stretching vibrations of the B-O bond in trigonal BO_3 units assigned between 1200–1600 cm^{-1}, The second region is assigned between 800–1200 cm^{-1}, arises from the stretching virational motions of the B-O bond in BO_4 tetrahedral units, while the third region is attributed to the B-O-B linkages bending vibrational movements within the borate network found at approximately around 700 cm^{-1}.

When analyzing the IR spectra of the fabricated borate materials, the FTIR assignments indicate that the bands at 1293 and 1203 cm^{-1} are associated with stretching vibrations of B-O in the BO_3^{3-} unit of orthoborates. Additional bands appearing at 736, 661, 610, 486, and 420 cm^{-1} are due to out-of-plane and in-plane bending, as well as lattice vibrations [27-31]. The absorption band at 3421 cm^{-1} belongs to the symmetric stretching mode of OH. The vibration bands of the products align well with those of $Mg_3(BO_3)_2$, with no significant changes observed upon the addition of varying amounts of dopant.

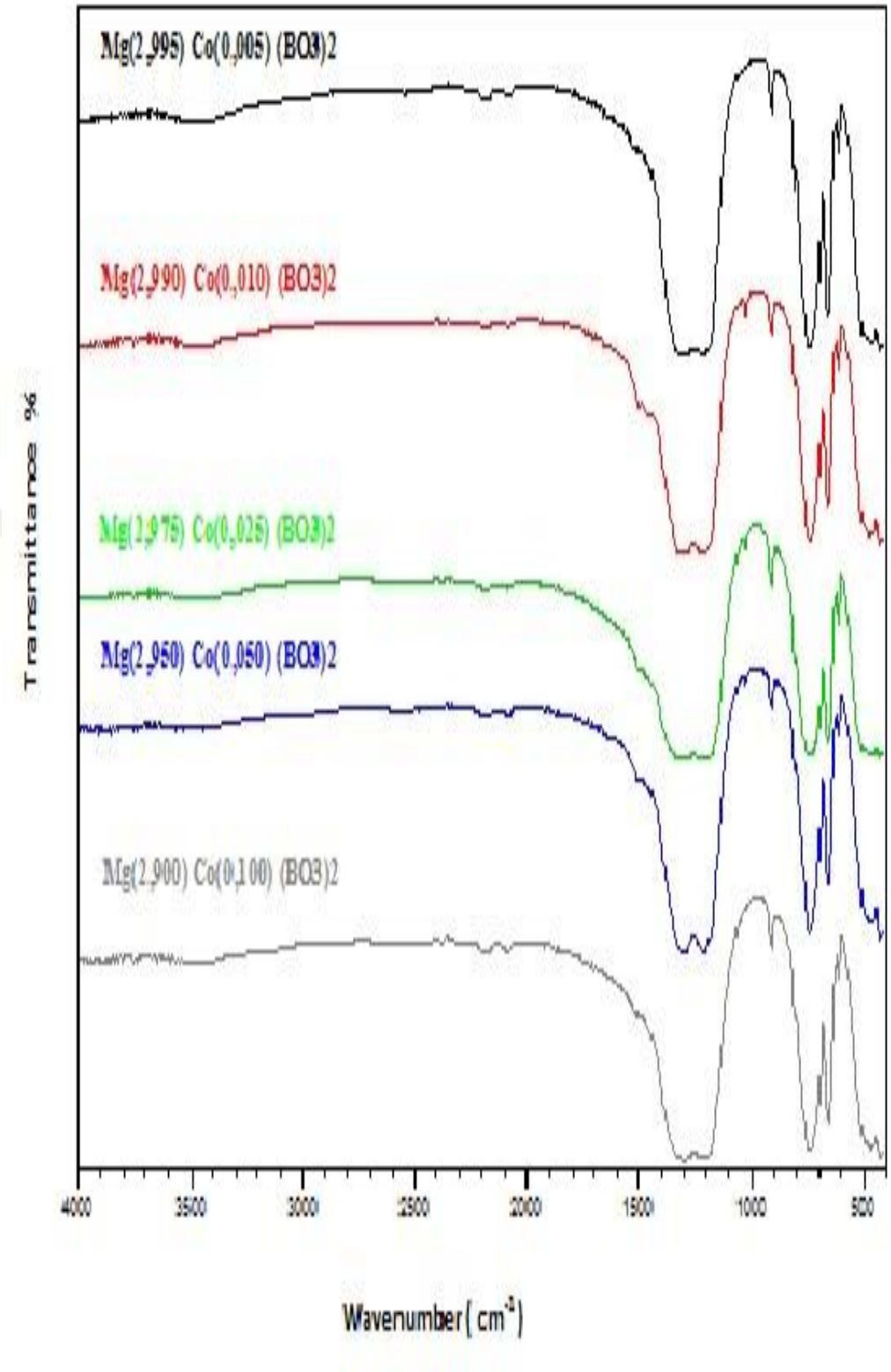

Figure 3.3. IR Spectra of $Mg_{(3-x)}\ Co_{(x)}(BO_3)_2$ (x = 0.005, 0.010, 0.025, 0.050, 0.100)

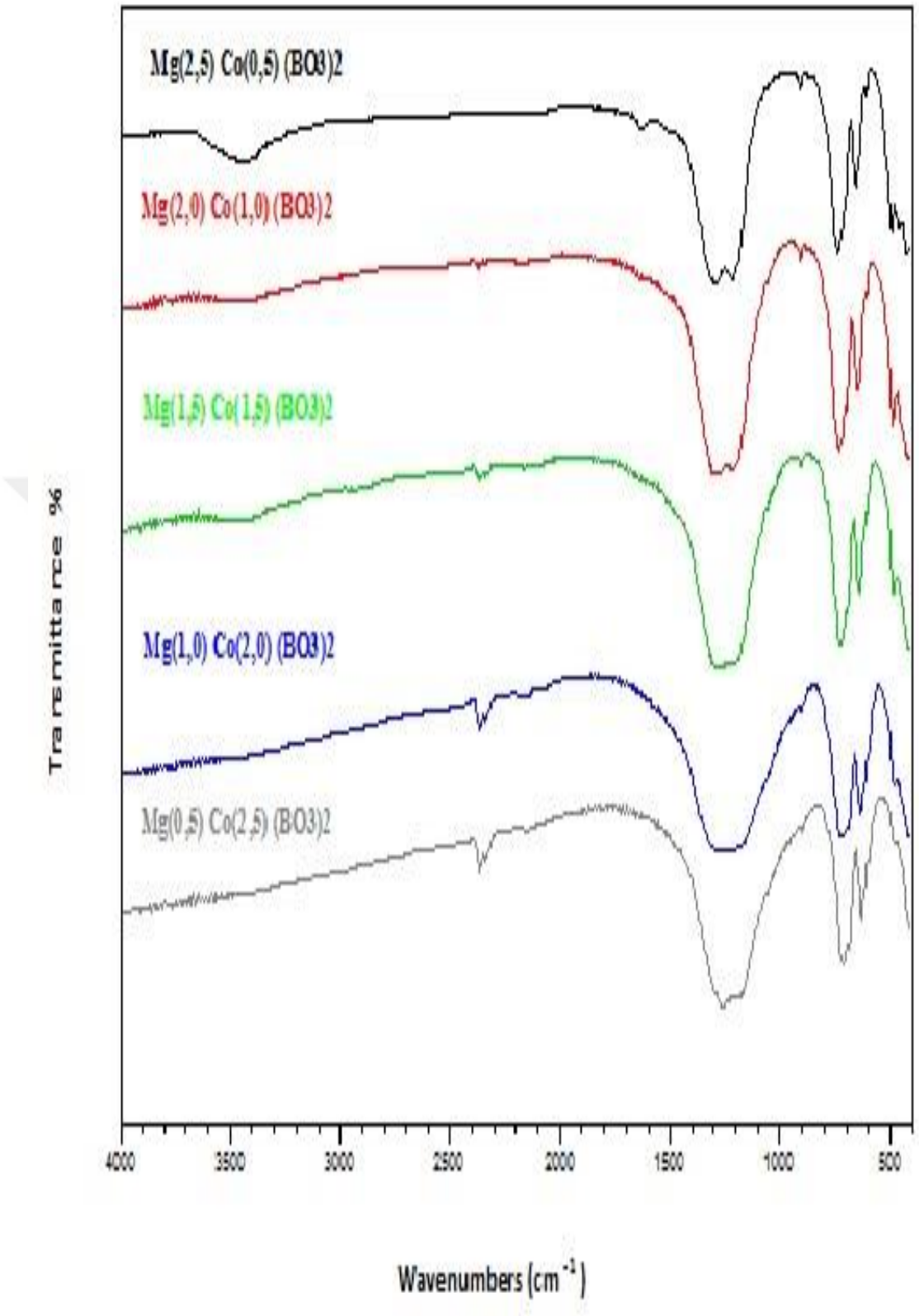

Figure 3.4. IR Spectra of $Mg_{(3-x)}Co_{(x)}(BO_3)_2$ (x = 0.5, 1.0, 1.5, 2.0, 2.5)

3.3 Optical Studies of the Co doped Magnesium borates

The optical properties of the samples prepared in this study were investigated using a UV–Vis spectrophotometer coupled with an integrating sphere for diffuse reflectance spectroscopic (DRS) measurements [26-28]. According to the results, the absorbance spectrum of all compounds showed two bands at 250 and 335 nm. The UV band positions for cobalt metal ion doped magnesium orthoborate samples slightly shift to the different wavelengths in comparison with the pure $Mg_3(BO_3)_2$ which can be attributed to the change in the acceptor level induced by the substitutional cobalt metal ion and the band-gap narrowing of $Mg_3(BO_3)_2$ with the cobalt metal ion dopants.

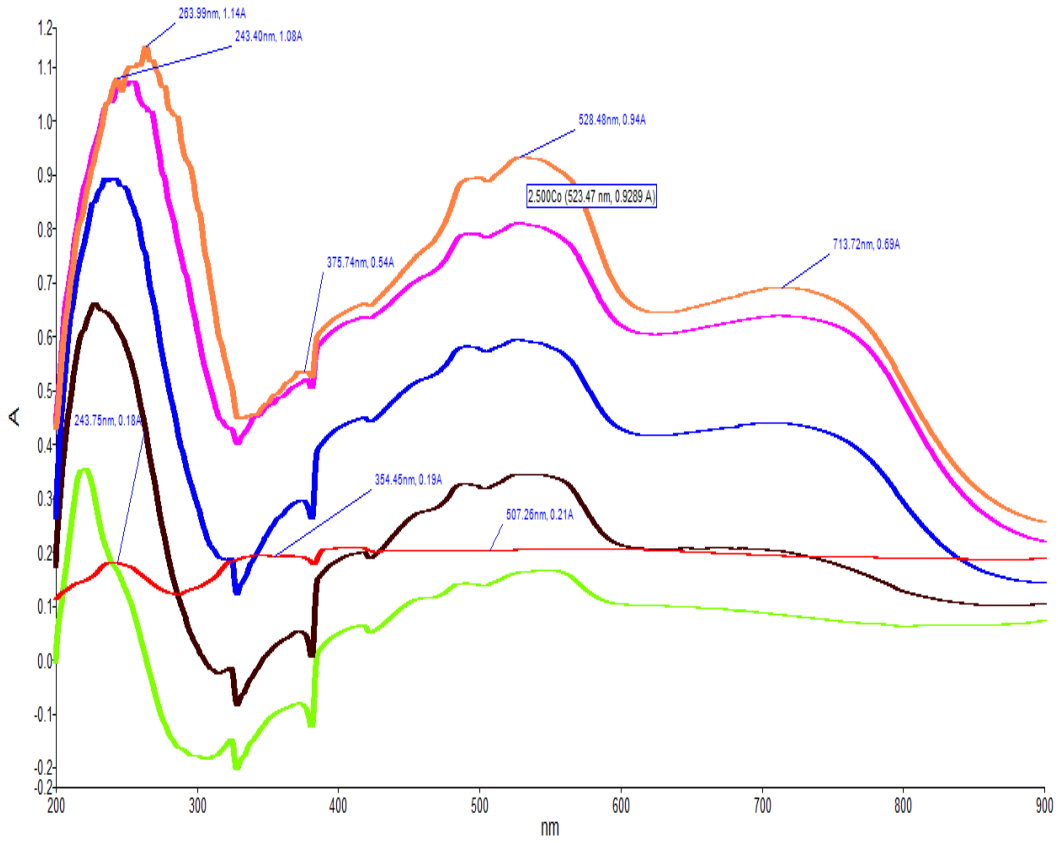

Figure 3.5. The Absorbance Spectra of $Mg_{(3-x)}Co_{(x)}(BO_3)_2$ (x = 0.005 , 0.010 , 0.025 , 0.050 , 0.100)

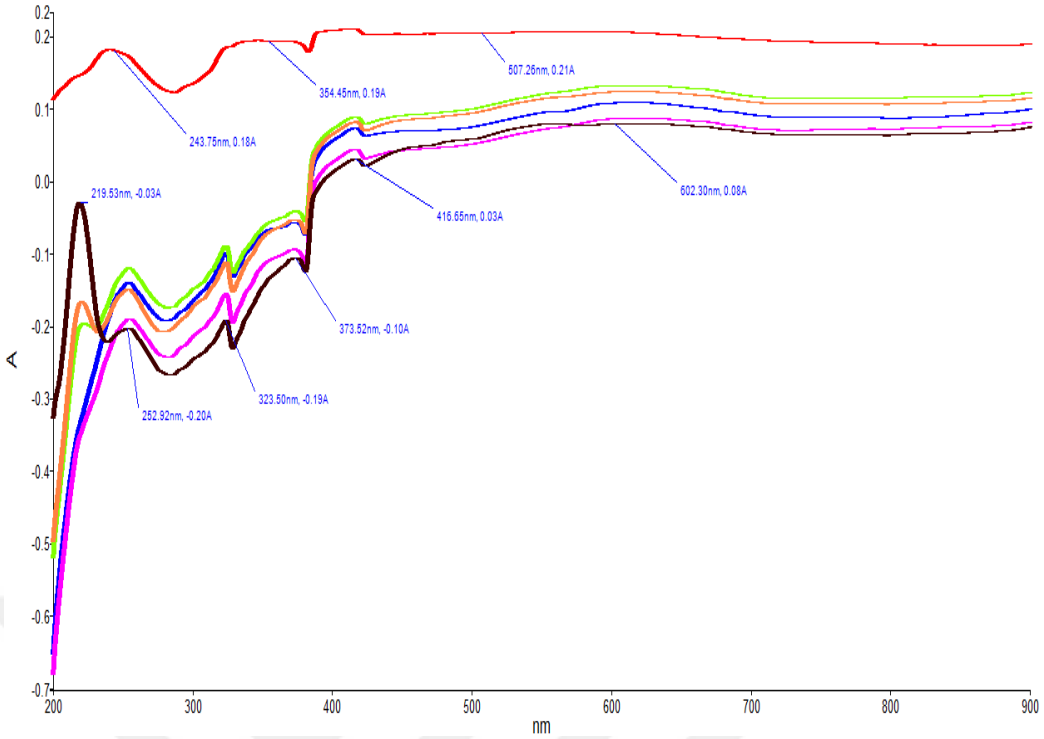

Figure 3.6. The Absorbance Spectra of $Mg_{(3-x)}Co_{(x)}(BO_3)_2$ (x = 0.5 , 1.0 , 1.5 , 2.0 , 2.5)

3.4 The Thermal Studies, (DTA/TG)

The DTA/TG curves [22] of cobalt doped magnesium orthoborate, $Mg_{3-x}Co_x(BO_3)_2$ (where x = 0, 0.01, 0.025, and 0.05), are presented as follows:

- The heating rate was maintained at 10°C per minute, with the temperature range extending from room temperature to 1400°C
- The curves demonstrate that these doped compounds maintain thermodynamic stability up to 1390°C, with only a minimal amount of weight loss observed within this temperature range.
- Additionally, as the cobalt content increases, the melting point of the doped samples varies.
- This confirms the presence of cobalt in the kotoite structure of magnesium orthoborate.

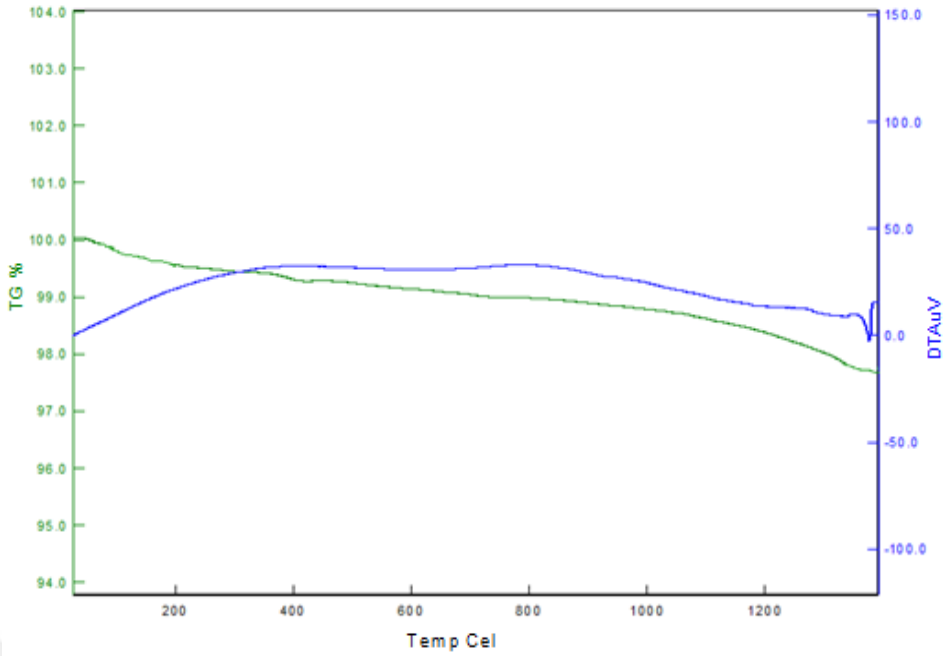

Figure 3.7. The DTA/TG curves of $Mg_3(BO_3)_2$

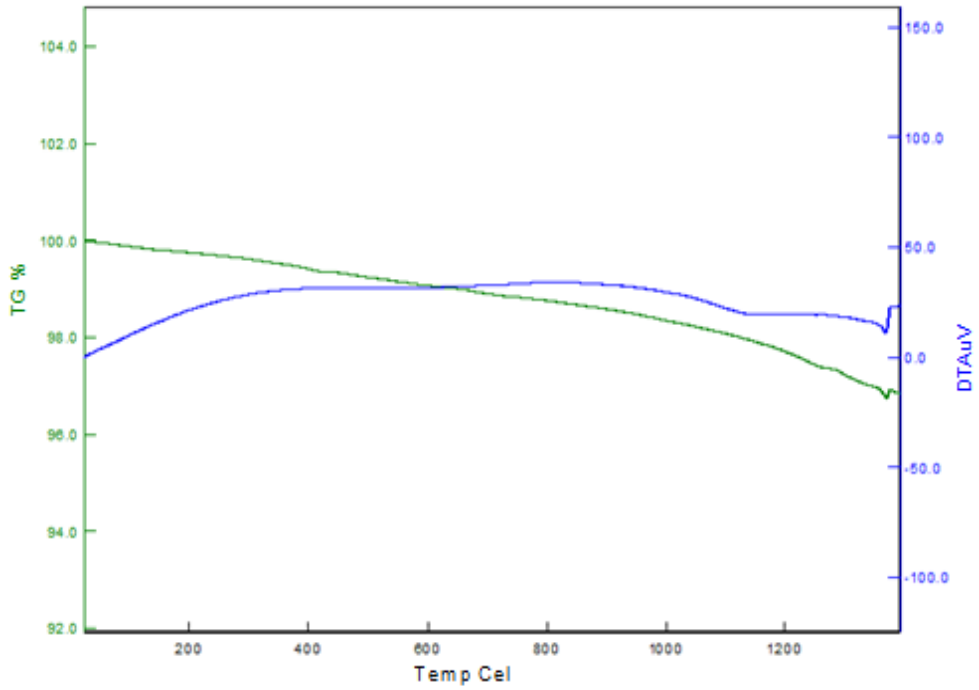

Figure 3.8. The DTA/TG curves of $Mg_{2.99}Co_{0.01}(BO_3)_2$

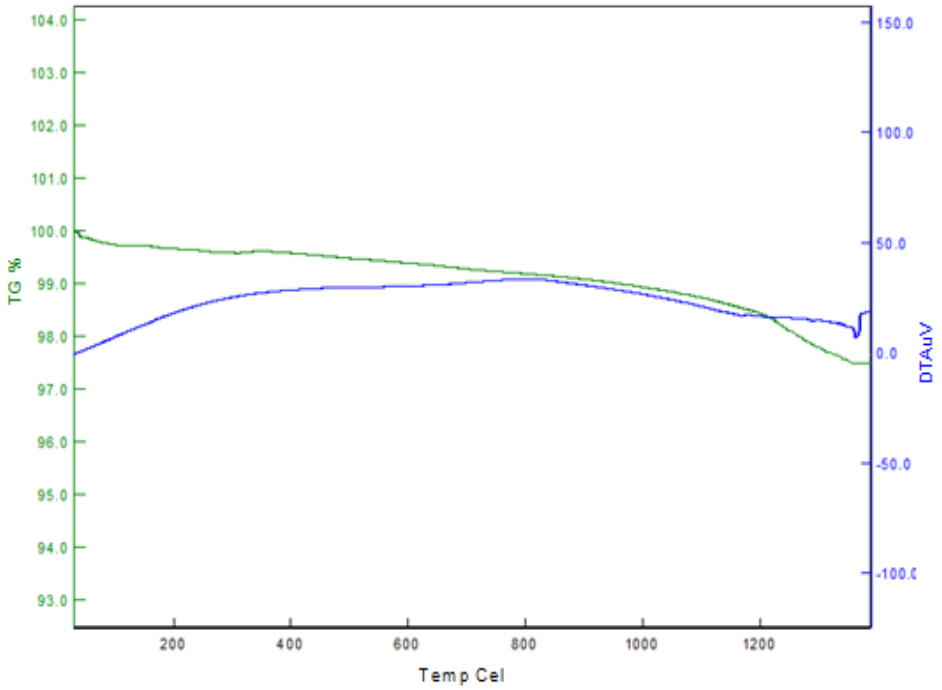

Figure 3.9. The DTA/TG curves of $Mg_{2.975}Co_{0.025}(BO_3)_2$

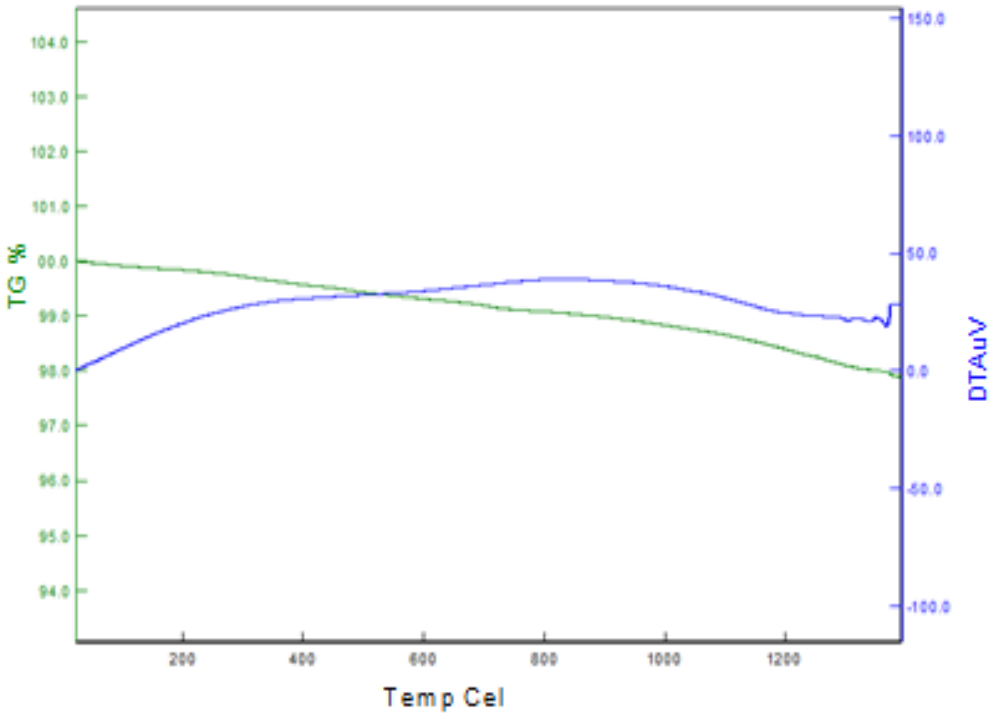

Figure 3.10. The DTA/TG curves of $Mg_{2.950}Co_{0.05}(BO_3)_2$

4. DISCUSSION

In this study, the magnesium orthoborate and Co(II) ion doped magnesium ortoborates were synthesized using a solid-state reaction technique at high temperatures. The starting materials, magnesium and cobalt nitrate hexahydrate and boric acid were chosen for their availability and suitability for producing orthoborate compounds. The solid state reaction was conducted at 900°C for 48 hours, which is a standard temperature for such conventional solid-state reaction method, allowing for the formation of the desired orthoborate structure. Introducing a 5% excess of boric acid ensures that sufficient boron is present to drive the reaction towards the formation of magnesium orthoborate. The products were then characterized using X-ray powder diffraction (XRD) and Fourier Transform Infrared Spectroscopy (FT-IR) to determine the crystal structure and band vibrations of the desired cobalt ion doped magnesium orthoborate compounds synthesized respectively.

The XRD analysis revealed that at lower cobalt concentrations, the predominant phase in the samples was magnesium orthoborate agreed with ICDD No: 75-1807. However, as the cobalt content increased, a shift in the phase composition occurred, with the formation of cobalt orthoborate becoming increasingly evident. This behavior highlights the concentration-dependent of dopant.

In the IR analysis, the data revealed that the bands at 1293 and 1203 cm^{-1} were associated with the stretching vibrations of B-O in the BO_3^{3-} unit of the orthoborate structure. Additional bands at 736, 661, 610, 486, and 420 cm^{-1} were assigned to out-of-plane and in-plane bending vibrational motions. The absorption band at 3421 cm^{-1} was attributed to the symmetric stretching mode of the OH group. These vibration bands were consistent with those of $Mg_3(BO_3)_2$, and no significant changes were observed upon the addition of varying amounts of the cobalt dopant, indicating that cobalt doping did not drastically alter the band vibrations of synthesized products.

The optical properties of the samples were also analyzed and revealed that the absorbance spectra of all the synthesized products showed two distinct bands at 250 nm and 335 nm. Notably, the UV band positions for the cobalt-doped magnesium orthoborate samples shifted slightly to different wavelengths compared

to single-phase $Mg_3(BO_3)_2$. These findings suggest that cobalt doping influences the optical properties of magnesium orthoborate.

The thermodynamic stability of the cobalt-doped magnesium orthoborate was assessed through Differential Thermal Analysis (DTA) and Thermogravimetric Analysis (TGA) [23]. The heating rate was maintained at 10°C per minute, with the temperature range extending from room temperature to 1400°C. The DTA/TG curves revealed that the doped compounds maintained thermodynamic stability up to 1390°C, with only minimal weight loss observed within this temperature range. Furthermore, the melting point of the doped samples varied with increasing cobalt content, suggesting that the presence of cobalt affects the melting behavior of the material. This confirms the addition of cobalt into the kotoite structure of magnesium orthoborate not only influences the material's optical properties but also enhances its thermal stability.

5. CONCLUSION

In this study, cobalt(II) ion doped magnesium orthoborates were successfully synthesized via the conventional solid-state reaction method using varying concentrations of cobalt ion as a dopant. The primary objective was to investigate the structural, vibrational, optical, and thermal properties of the synthesized ceramic borate materials, with particular attention to the effects of cobalt incorporation into the magnesium orthoborate matrix.

Structural characterization was carried out using X-ray diffraction (XRD). At low cobalt doping levels, the diffraction patterns matched exclusively with magnesium orthoborate, $Mg_3(BO_3)_2$, indicating the formation of a pure single-phase orthoborate material. The absence of secondary phases suggests that cobalt ions are homogeneously incorporated into the magnesium orthoborate, $Mg_3(BO_3)_2$ lattice without disrupting the host crystal structure. This demonstrates that the kotoite-type structure can accommodate a limited amount of cobalt substitution. However, beyond a certain doping threshold, additional diffraction peaks associated with cobalt orthoborate, $Co_3(BO_3)_2$, appeared, signaling the onset of phase separation. This shift from single-phase to multiphase composition reflects the limited solubility of cobalt ions within the magnesium orthoborate lattice, with excess cobalt amount crystallizing into its own phase once the solubility limit is exceeded.

These findings emphasize the critical role of dopant concentration in maintaining structural homogeneity and phase purity. To further probe the local structural environment, Fourier-transform infrared (FTIR) spectroscopy was employed. Across all cobalt concentrations, the FTIR spectra exhibited distinct absorption bands characteristic of trigonal planar BO_3 units, which remained consistent in both position and intensity. This spectral invariance indicates that cobalt incorporation does not significantly alter the local bonding environment of the borate groups. The symmetric and asymmetric B–O stretching vibrations remained unaffected, confirming that the borate substructure and overall lattice symmetry are preserved despite metal ion substitution.

The consistency of the FTIR spectra supports the XRD results, collectively demonstrating that cobalt ions integrate into the magnesium orthoborate lattice

without causing detectable perturbations to either the long-range crystalline order or the local bonding structure. Even at increased doping levels, the kotoite-type structure retains its integrity, with no evidence of significant band broadening or peak shifting in the FTIR spectra. This dual confirmation underscores the structural compatibility of cobalt ions within the magnesium orthoborate, $Mg_3(BO_3)_2$ framework.

In addition to structural and vibrational studies, optical and thermal properties were explored. Ultraviolet-visible (UV-Vis) spectroscopy revealed a slight redshift in the absorption edge for cobalt(II) ion doped samples compared to undoped magnesium orthoborate, $Mg_3(BO_3)_2$. This shift indicates minor modifications in the electronic structure due to cobalt substitution, which may influence the optical band gap and enhance the material's potential in optoelectronic or photonic applications.

Thermal stability was assessed through thermogravimetric-differential thermal analysis (TG-DTA). All samples exhibited high thermal resistance, with no significant mass loss observed up to approximately 1390 °C. Notably, this thermal behavior was consistent across all cobalt concentrations, indicating that doping does not compromise the material's thermal robustness.

In conclusion, the successful incorporation of cobalt(II) ions into the magnesium orthoborate matrix has been demonstrated without sacrificing structural order, vibrational stability, or thermal resistance. While the optical properties exhibited subtle yet meaningful changes, the borate framework and kotoite-type crystal structure remained fundamentally intact. These results provide a promising foundation for further development of cobalt ion doped orthoborate materials in advanced functional applications, particularly in high-temperature and optoelectronic technologies.

REFERENCES

1. Greenwood, N. N., Earnshaw, A., 1998, Chemistry of The Elements, Butterword Heinemann Pub., Great Bratain.
2. Chatterjee, K. K., 2007, Uses of Metals and Metallic Minerals, New Age International Publishers, New Delhi.
3. Kar, Y., Şen, N., Demirbaş, A., 2006. Boron Minerals in Turkey, Their Application Areas and Importance for the Country's Economy. Minerals & Energy, 3–4, 2–10.
4. Barth, S., 1998. Application of boron isotopes for tracing sources of anthropogenic contamination in ground water. Pergamon, 32, 3, 685-690.
5. Richard, B., 2006, The Elements Boron, Newyork: Marshall Cavendish Benchmark pub., 4-6.
6. Culver, B. D., Smith, R. G., Brotherton, R. J.,Strong, P. .L., Gray, T. M., 1994, Chapter 44:Boron. In: Clayton, G. D., Clayton, F. E. (eds).Patty's industrial hygiene and toxicology, NewYork, John Wiley and Sons, vol 2, part 1
7. Christ, C. L., and Clark, J. R, 1977, A Crystal-Chemical Classification of Borate Structures with Emphasis on Hydrated Borates. Physics and Chemistry of Minerals 2, 59-87
8. Velchuri, R., Kumar, B. V., Devi, V. R., Prasad, G., Prakash, D. J., Vithal, M., 2011, Preparation and characterization of rare earth orthoborates, $LnBO_3$ (Ln = Tb, La, Pr, Nd, Sm, Eu, Gd, Dy, Y) and $LaBO_3$:Gd, Tb, Eu by metathesis reaction: ESR of $LaBO_3$:Gd and luminescence of $LaBO_3$:Tb, Eu. Materials Research Bulletin, 46, 1219–1226.
9. Frost, R. L., and Xi, Y. 2012**,** Vibrational spectroscopy of the borate mineral kotoite $Mg_3(BO_3)_2$, Spectrochimica Acta Part A: Molecular and Biomolecular Spectroscopy, 1386-1425 (12) 01127-4.
10. Stewart, D. A., 2009, Oxide layer boron leads to reduced symmetry spin filtering magnetic tunnel junctions. arXiv:0904.4475v1 [cond-mat.mtrl-sci].
11. Rahaman, M. N., 2003, Ceramic Processing and Sintering. 2nd edution, CRC press, USA. Chapter 2, 61-92.
12. West, R. A., 1990, Solid State Chemistry and Its Applications. 5th edution, John Willey & Sons press, USA. Chapter 2, p.5,6.
13. Rao, C. N. R., Gopalakrishnan, J., 1997, New Directions in Solid State Chemistry. 2nd edition, Cambridge University press, USA. Chapter 3, p.125.
14. Smart, L. E., Moore, E. A., 2005, Solid State Chemistry, 3th edution, CRC press Taylor & Francis Group, England. Chapther 3, p. 148-152.
15. Segal, D., 1997, Chemical synthesis of ceramic materials. http://pubs.rsc.org | doi:10.1039/A700881C
16. Beatty Richard, 2006, The Elements Boron, Newyork: Marshall Cavendish Benchmark Pub., p. 4-6
17. Chaminade J. P., Gravereau P., Jubera V., Fouassier C., 1999, "Discovery of a New Group of Lithium Rare-Earth Oxyborates, $LiLn_6O_5(BO_3)_3$ (Ln: Pr-Tm): Structural Analysis of the Gadolinium Variant $LiGd_6O_5(BO_3)_3$," Journal of Solid State Chemistry, 146, pp. 189-196.
18. Zhang G., Wu Y., Fu P., Wang G., Liu H., Fan G., Chen C., 2002, "A Novel Sodium Samarium Borate: $Na_3Sm_2(BO_3)_3$," Journal of Physics and Chemistry of Solids, 63, pp. 145-149.
19. Wu L., Zhang Y., Kong Y. F., Sun T. Q., Xu J. J., Chen X. L., 2007, "Structural Identification of New Orthoborates $NaMgBO_3$: A Potential Birefringent Crystal," Inorganic Chemistry, 46, pp. 5207-5211.
20. Anantharamulu N., Vijaya Kumar B., Rama Devi V., Vithal M., 2007, "Synthesis, Characterization, and Spectral Investigations of Cr1-xEuBO3 (x=0, 0.01, 0.05)," Materials Chemistry and Physics, 108, pp. 319-324.
21. Latha Kumari L., Li W. Z., Kulkarni S., Wu K. H., Chen W., Wang C., Vannoy C. H., Leblanc R. M., 2010, "Impact of Surfactants on the Structural and Morphological Features of Magnesium orthoborate Hydroxide Nanowhiskers Synthesized via a Hydrothermal Approach," Nanoscale Research Letters, 5, pp. 149–157.

22. Cai G. M., Tao X. M., Su L. M., Zheng F., Yi D. Q., Chen X. L., Jin Z. P., 2011, "Exploring the Structure, Thermal Stability, and Properties of $Li_3Sc(BO_3)_2$," Journal of Solid State Chemistry, 184, pp. 115–122.
23. Péter A., Polgar K., Toth M., 2012, "Development and Crystallization of Lithium-Yttrium Orthoborate $Li_6Y(BO_3)_3$ Phase," Journal of Crystal Growth, 346, pp. 69–74.
24. Berger S. V., 1949, "Crystallographic Analysis of Isomorphic Orthoborates of Cobalt and Magnesium," Acta Chemica Scandinavica, 3, pp. 660-675.
25. Effenberger H., Pertlik F., 1984, "Refinement of Crystal Structures of Isotypic Compounds $M_3(BO_3)_2$ with M = Mg, Co, and Ni (Kotoite Structure Type)," Zeitschrift Für Kristallographie, 166, pp. 129-140.
26. Akhamanova, M. V., 1961, "Structural Study of Natural Borates Using Infrared Absorption Spectroscopy," Zhurnal Strukturnoi Khimii, 3(1), pp. 28-34.
27. Ternane, R., Cohen-Adad, M. T., Panczer, G., Goutaudier, C., Kbir-Ariguib, N., Trabelsi-Ayedi, M., Florian, P., Massiot, D., 2002, "Incorporation of Boron into Hydroxyapatite: Synthesis and Structural Characterization," Journal of Alloys and Compounds, 333, pp. 62–71.
28. Lakshminarayana, G., Buddhudu, S., 2005, "Spectroscopic Evaluation of Cu^{2+}-Doped Glasses Based on B_2O_3–ZnO–PbO," Spectrochimica Acta Part A, 62, pp. 364–371.
29. Tukia, M., Hölsä, J., Lastusaari, M., Niittykoski, J., 2005, "Eu^{3+}-Doped Rare Earth Orthoborates (RBO_3, R = Y, La, Gd) Prepared by Combustion Synthesis," Optical Materials, 27, pp. 1516–1522.
30. Chen, A. M., Gu, P., Ni, Z. M., 2012, "Fabrication of 3D Flower-Like Magnesium orthoborate Microspheres Assembled from Nanosheets via PVP-Assisted Method," Materials Letters, 68, pp. 187–189.
31. Altuntaş Öztas, N., Erdoğan, H., 2009, "Magnesium Pyroborate: Synthesis and Characterization Using Solution Combustion and Traditional Ceramic Techniques—A Comparative Study," Zeitschrift Für Anorganische Und Allgemeine Chemie, pp. 1626–1632.